Active Layer Thickness Estimation from X-Band SAR Backscatter Intensity

Barbara Widhalm[1], Annett Bartsch[1,2], Marina Leibman[3,4], and Artem Khomutov[3,4]

[1]Zentralanstalt für Meteorologie und Geodynamik, 1190 Vienna, Austria
[2]Vienna University of Technology, 1040 Vienna, Austria
[3]Earth Cryosphere Institute, Russian Academy of Sciences, Tyumen 625000, Russia
[4]Tyumen State University, Tyumen 625006, Russia

Correspondence to: Barbara Widhalm (barbara.widhalm@zamg.ac.at)

Abstract. The active layer above the permafrost, which seasonally thaws during summer is an important parameter for monitoring the state of permafrost. Its thickness is typically measured locally. A range of methods, which utilize information from satellite data exist. Their applicability has been demonstrated mostly for shallow depths below 70 cm. Some permafrost areas including central Yamal are characterized by higher Active Layer Thickness (ALT). The relationship between ALT and X-Band SAR backscatter of TerraSAR-X has been investigated in order to explore the possibility of delineating ALT on a continuous and larger spatial coverage in this area. This study shows that the mutual dependency of ALT and TerraSAR-X backscatter on land cover types induces a connection of both parameters. A range of 5 dB can be observed for an ALT range of 100 cm (40 - 140 cm) and an R² of 0.66 has been determined over the calibration sites. An increase of ALT with increasing backscatter can be especially determined for ALT > 70 cm. The RMSE over a comparably heterogeneous validation site with maximum ALT of > 150 cm is in the range of 20 - 22 cm. Deviations are larger for measurement locations with mixed vegetation types.

1 Introduction

Permafrost is defined as soil or rock that remains at or below 0°C for two or more consecutive years (Harris et al., 1988) and currently underlies some 25 % of the Earth's land surface (Huggett, 2007). Due to global warming extensive areas where permafrost is presently within a degree or two of the melting point could be destabilized (Smith, 1990). At global scale, increased ground temperatures could facilitate further climatic changes by releasing greenhouse gases that are currently sequestered in the upper layer of permafrost by increasing the annual thaw depth (Kane et al., 1991; Gomersall and Hinkel, 2001; Shiklomanov and Nelson, 1999). The top layer of ground subject to annual thawing and freezing in areas underlain by permafrost is defined as the active layer (Permafrost Subcommittee, 1988). In this layer most ecological, hydrological and biochemical activities take place (Kane et al., 1991; Brown et al., 2000). Furthermore it is an essential climate variable to monitor permafrost regions (Schaefer et al., 2015), making it not only an important factor at regional but also global scale. The active layer thickness (ALT) is predominately controlled by ambient temperature, but is also influenced by insulation layers such as snow cover and vegetation, slope, drainage, soil type, organic layer thickness and water content (Leibman, 1998; Shiklomanov and Nelson, 1999; Hinkel and Nelson, 2003; Kelley et al., 2004; Melnikov et al., 2004; Vasiliev et al., 2008). Due to the interaction

between these often highly localized surface and subsurface factors, ALT can vary substantially over short lateral distances (Shiklomanov and Nelson, 1999; Leibman et al., 2012).

Near-surface permafrost area is projected to decrease within the next century (IPCC, 2013). Changes in active layer thickness have been already observed for Yamal (Leibman et al., 2015). Active layer thickness spatial patterns are unknown outside of
5   the sites with in situ measurements.

Analytical procedures exist to estimate ALT, such as the Stefan solution (Harlan and Nixon, 1978) or the Kudryavtsev equation. While the Stefan solution links the seasonal thaw depth to the accumulated surface thawing-degree days, the Kudryavtsev equation accounts for the effects of snow cover, vegetation, soil moisture, thermal properties, and regional climate (Kudryavtsev et al., 1974; Yershov, 1998; Shiklomanov and Nelson, 1999). These methods, although accurate, are labour intensive and
10   limited in spatial coverage (Gangodagamage et al., 2014). While traditional in situ measuring methods like probing with metal rods are very inefficient at regional scale, remote sensing holds a great potential.

ALT can also be derived by empirical relationships between probe measurements and a physical attribute measurable by remote sensing (Schaefer et al., 2015). Especially optical data have been used to retrieve vegetation characteristics (see Table 1). A combination with derivatives of digital elevation models has been shown of added value (Peddle and Franklin, 1993;
15   Leverington and Duguay, 1996; Gangodagamage et al., 2014). Recently, subsidence rates have been used as input for modelling ALT (Schaefer et al., 2015). Most of these studies were conducted in areas with shallow ALT (for instance in Schaefer et al. (2015) the average ALT was 30 - 40 cm). Deeper active layers were modeled by analytical approaches (e.g., Sazonova and Romanovsky, 2003) or by incorporating only a few ALT classes (e.g., Leverington and Duguay, 1996). Application of high resolution optical satellite data has been shown possible in combination with high resolution digital elevation data from airborne
20   measurements. Such applications are however very limited in spatial extent.

Most previous remote sensing approaches (Leverington and Duguay, 1996; McMichael et al., 1997; Sazonova and Romanovsky, 2003; Schaefer et al., 2015) have utilized data with spatial resolutions of 30 m and coarser and are limited to ALT less than 70 cm (see Table 1). Many regions such as the Yamal peninsula are however characterized by a larger ALT range.

Investigations have been made using the Normalized Difference Vegetation Index (NDVI) (McMichael et al., 1997; Kelley
25   et al., 2004), digital elevation data and land-cover classes (Nelson et al., 1997; Peddle and Franklin, 1993). Synthetic Aperture Radar has been exploited using interferometric analyses (InSAR, provides seasonal ground subsidence) in combination with soil properties to estimate ALT (Schaefer et al., 2015). The utility has been demonstrated for average thaw depths of 30-40 cm and applicable to soils which are saturated all summer. Outside of such sites, ALT is underestimated. This would apply to many parts of the Yamal region. Previous tests in that region indicate that ALT below 70 cm, 70 - 100 cm and above 100 cm
30   can be distinguished using NDVI (Leibman et al., 2015).

SAR backscatter intensity has so far not been investigated for ALT estimation. Radar backscatter at X-band is also related to vegetation coverage, especially shrubs (Duguay et al., 2015), similarly to the NDVI. The overall backscatter intensity of a certain surface area is also influenced by surface roughness with respect to the wavelength (3.1 cm). In this study we hypothesize that there is a relationship between local ALT and X-band measurements. In situ records from several sites in the proximity of
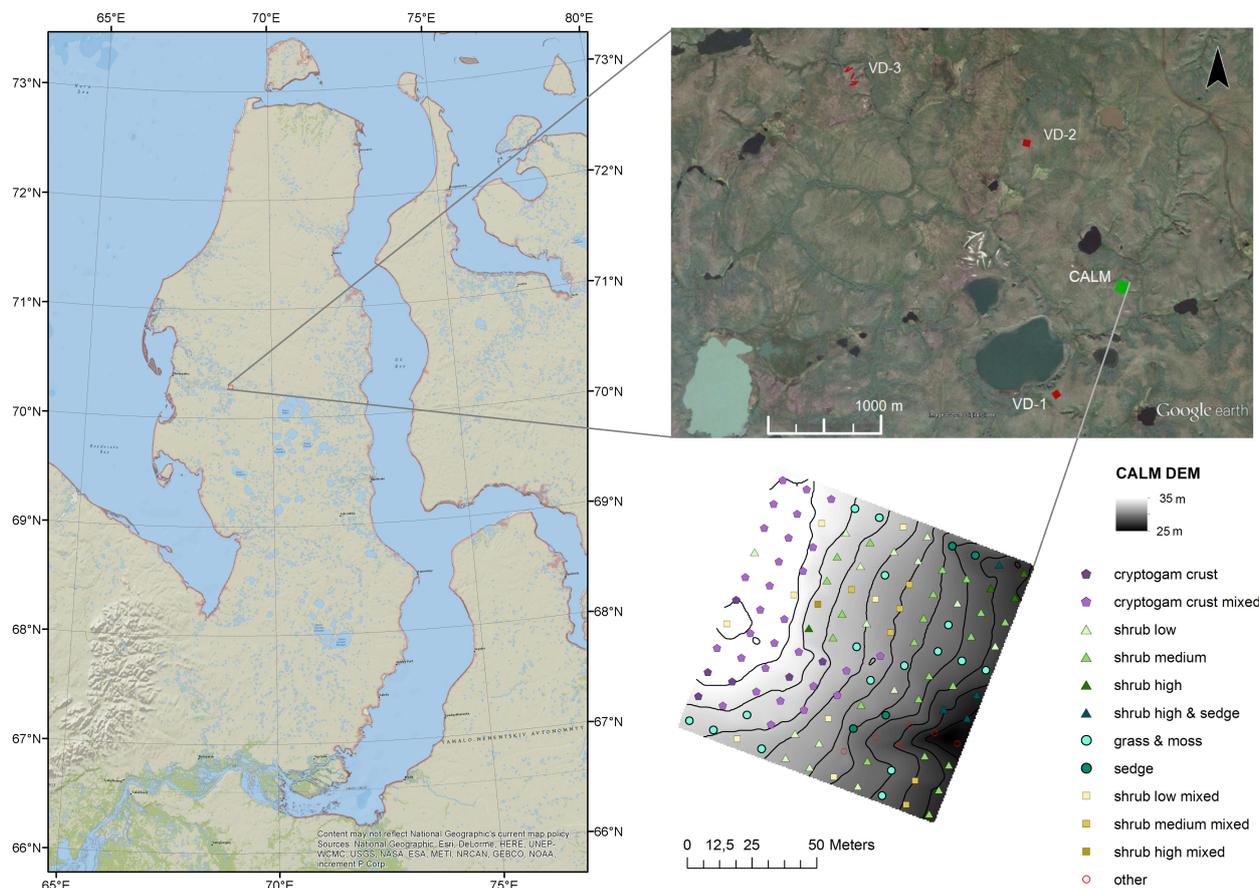
Figure 1. Location of the study area within the Yamal peninsula and CALM grid DEM with land cover information (Sources left: ArcMap Basemap: National Geographic, Esri, DeLorme, HERE, UNEP-WCMC, USGS, NASA, ESA, METI, NRCAN, GEBCO, NOAA, increment P Corp. Source top right: Google Earth, Image © 2016 Digital Globe)

a long-term monitoring site on Yamal have been used and results are discussed with respect to previous approaches which use remotely sensed information as proxy for ALT.

2   Study area and datasets

2.1   The Vaskiny Dachi monitoring site

5   The Vaskiny Dachi research station (70°20'N, 68°51'E) was established in 1988 and is situated in the central Yamal Peninsula in a system of highly-dissected alluvial-lacustrine-marine plains and terraces. It is located within a region of continuous permafrost where tundra lakes and river flood plains are the most prominent landscape features (Leibman et al., 2015). Dense

Table 1. Studies which used satellite data for determination of active layer thickness (ALT): type of satellite data, accuracy and active layer ranges

Reference	remotely sensed data	ALT measurement	resolution	ALT	accuracy
Peddle and Franklin (1993)	SPOT imagery (land cover) and photogrammetric DEM	in situ soil probing at regular intervals throughout field sample sites of 60 x 60 m	20 m	classes: < 25 cm; 25 cm - 50 cm; > 50 cm; no permafrost	79% agreement for the four classes
Leverington and Duguay (1996)	Landsat Thematic Mapper (NDVI, land cover) and DEM data	pit measurements supplemented by three ground probing measurements in 5 m intervals in four directions at each site	30 m	classes: < 70 cm; 70 cm - 150 cm; > 150 cm	93% agreement for the three ALT classes
McMichael et al. (1997)	Landsat Thematic Mapper and handheld radiometer (NDVI)	median of five ground probing measurements at each sample point	30 m	average: < 35 cm	No relationship between NDVI and ALT on the North Slope of Alaska in areas with little variation in relief. In areas where topography strongly controls the flow and redistribution of water, NDVI did account for approximately 40% of the variability
Gangodagamage et al. (2014)	LiDAR (local slope and landscape curvature) and Worldview-2 (NDVI)	probing along transects of diverse length and at various intervals	2 m	20 -70 cm	$R^2 = 0.76$ and RMSE ± 4.4 cm
Schaefer et al. (2015)	Subsidence from multiannual Phased Array type L-band Synthetic Aperture Radar (PALSAR)	average of calibrated Ground Penetrating Radar (GPR) measurements within each pixel (~ 40 traces per pixel); probe measurements at two CALM sites (1 x 1 km grid with 100 m interval, 10 x 10 m plot random point placement)	~ 30 m	average: 30 - 40 cm; < 40 cm in areas outside of drained lake basins	~ 76% of the study area within uncertainty of the used Ground Penetrating Radar and probing data (~ 8 cm)

dwarf shrubs (Betula nana) are widespread on the watersheds. Well-drained hilltops are occupied by dwarf shrub-moss-lichen communities. On gentle poorly drained slopes, low shrubs and dwarf shrubs are well developed and mosses predominate. On convex tops and windy hill slopes, shrub-moss-lichen communities with spot-medallions are predominant. River valleys, thermocirques, and landslide cirques with thick snow cover are characterized by willow thickets. Sedge and sphagnum bogs and flat-topped polygonal peatlands are common on flat and concave (saddles) surfaces of watersheds and terraces, in the river valley bottoms, on low lake terraces and in other depressions (Khomutov and Leibman, 2014).

The study area is characterized by continuous permafrost. ALT ranges between 40 cm in peat and up to 120 cm on sandy, poorly vegetated surfaces (Melnikov et al., 2004; Vasiliev et al., 2008; Leibman et al., 2011, 2012). There are extremes observed on high-center sandy polygons, which can be 1–1.5 m high and up to 10 m in diameter, with active layer exceeding 2 m. Spatial changes in ground temperature are controlled by the redistribution of snow which is resulting from strong winds characteristic for tundra environments and the highly dissected relief of Central Yamal (Dvornikov et al., 2015). Lowest ground temperature is characteristic for hilltops with sparse vegetation where snow is blown away. The warmest are areas with high willow shrubs, due to the retention of snow, found on slopes, in valleys and lake depressions. While the spatial distribution of ALT depends on lithology and surface covers, temporal fluctuations are controlled by ground temperature, summer air temperature and summer precipitation (Leibman et al., 2015).

2.2 In situ measurements

In 1993 a Circumpolar Active Layer Monitoring (CALM) site was established at Vaskiny Dachy, placed on the top and slope of a highly dissected plain, affected by landslides, with sandy to clayey soils. The CALM program, designed to observe the response of the active layer and near-surface permafrost to climate change, currently incorporates more than 100 sites. The International Permafrost Association serves as the international facilitator for the CALM network, which is now part of the WMO Global Terrestrial Network for Permafrost (GTN-P) (Brown et al., 2000).

Within the Greening of the Arctic (GOA) project of the International Polar Year (IPY), which was funded by NASA's Land-Cover Land-Use Change (LCLUC) program, three additional monitoring sites were established in the Vaskiny Dachi area (Walker et al., 2009). Study sites were established within areas with more or less homogeneous vegetation. The site Vaskiny Dachi-1 (VD-1) has clay soils and the vegetation is heavily grazed sedge, dwarf-shrub-moss tundra. Soils at Vaskiny Dachi-2 (VD-2) are a mix of sand and clay, its vegetation is heterogeneous, but dominated by dwarf birch, small reed grass and sedge, cowberries and mosses. At Vaskiny Dachi-3 (VD-3) the soils are sandy and the vegetation is a dry dwarf-shrub-lichen tundra (Walker et al., 2009).

The ALT is measured by a metal probe according to CALM protocol. This involves a late season mechanical probing, in this case late August, when ALT is near its end-of-season maximum. A 1 cm diameter graduated steel rod is inserted into the soil to the depth of resistance to determine the depth of thaw (Brown et al., 2000).

ALT is measured at a spacing of 10 m within the 100 x 100 m grid at the CALM site, resulting in 121 measuring points. The VD sites feature 5 transects respectively. At VD-1 and VD-2 these transects form grids of 50 x 50 m. Transects are 12.5 m apart and ALT is measured every 5 m, resulting in 55 measurement points per site. The transects at VD-3 are arranged to areas of

homogeneous vegetation (Walker et al., 2009). The site of VD-3 features higher ALT values, most likely because of the present sandy soils, which yield a greater conductivity and water permeability (higher convective heat exchange). The CALM grid site is far more heterogeneous than the other VD sites and holds patches of dry cryptogam crust, grasses and mosses, low and high shrubs as well as some wet sedge spots. Cryptogam crust is encountered at the concave hilltop, while high shrubs were mostly located at the landslides (Figure 2). Here, ALT is locally higher due to high salinity of clayey deposits which contain no ice under negative temperature and do not resist to probing.

A dedicated vegetation survey of each CALM grid point was carried out in August 2015. The dominant vegetation cover within a 3 x 3 m area was determined. The following classes are distinguished: Cryptogam crust, low shrubs (< 15 cm), medium shrubs (15 -30 cm), high shrubs (> 30 cm), grass and moss as well as a class where sedges dominate and classes of mixed vegetation. Further information on vegetation has been collected outside of the ALT measurement sites in August 2014. Over 60 points were registered but only 36 of these points could be further used because of low homogeneity with respect to the spatial resolution of the satellite data. This survey included the most dominant classes of the region: low shrubs (< 20 cm), medium shrubs (20 -60 cm), high shrubs (> 60 cm), Cryptogam crust, and a mixture of grasses and sedges.

Furthermore moisture measurements were conducted at the CALM grid. The Delta-T Wet Sensor with HH2 handheld was used to measure the moisture content of the top 5 cm at each grid point on three dates in August 2015.

2.3 TerraSAR-X acquisitions

The German national SAR-satellite system TerraSAR-X is based on a public-private-partnership agreement between the German Aerospace center DLR and EADS Astrium GmbH. It was launched in June 2007 and started its operational service at the beginning of 2008 (DLR, 2009). The satellite flies in a sun-synchronous, dawn dusk orbit with an 11-day repeat period. TerraSAR-X features an advanced high-resolution X-Band Synthetic Aperture Radar with a centre frequency of 9.65 GHz corresponding to a wavelength of about 3.1 cm. TerraSAR-X operates in Spotlight-, Stripmap- and ScanSAR Mode with various polarizations. In this study HH (horizontally sent and horizontally received) polarized images of Stripmap mode were used, which image strips of 30 km width and a maximum length of 1.5 km and 3 m resolution (Werninghaus et al., 2004).

All images were obtained as SSC (Single Look Slant Range Complex). Available data have been acquired in the same ascending orbit and beam (incidence angle range 27.3° - 30.3°).

The TanDEM-X mission is an extension of the TerraSAR-X mission, coflying a second satellite of nearly identical capability in a close formation. This enables the acquisition of highly accurate cross- and along-track interferograms without the inherent accuracy limitations imposed by repeat-pass interferometry due to temporal decorrelation and atmospheric disturbances (Krieger et al., 2007). In this study the TanDEM-X Intermediate DEM (IDEM, ∼ 12 m pixel spacing, < 10 m absolute horizontal and vertical accuracy) was used for terrain correction, which, compared to the final TanDEM-X DEM product, might have limitations with respect to product quality and completeness (DLR).

2.4 Landsat data

Landsat 8, launched in 2013, is a NASA (National Aeronautics and Space Administration) and USGS (Department of the Interior U.S. Geological Survey) collaboration, which extends the 40 year Landsat record. It carries two sensors, the Operational Land Imager (OLI) and the Thermal Infrared Sensor (TIRS), which spectral bands remain comparable to the Landsat 7 ETM+

5 and operate in the visible, near-infrared, short wave and thermal infrared. Landsat 8 flies in a near-polar, sun-synchronous 705 km circular orbit and acquires data in 185 km swaths segmented into 185 km x 180 km scenes. For this study two Level 1 terrain-corrected (L1T) scenes of 22nd July 2014 and 10th August 2015 were obtained in order to calculate NDVI (spatial resolution 30 m) and compare the already established approach of using NDVI for ALT delineation to the in this study introduced approach.

3 Methodology

In Microwave Remote Sensing the radar backscatter is dependent on sensor parameters like incidence angle, polarization and wavelength and also on geometric parameters such as surface roughness and vegetation structure, as well as soil properties. Shorter wavelengths do not penetrate as much as longer wavelengths into vegetation and soil, therefore short wavelengths like X-band rather yield information about the upper layers of vegetation (Ulaby et al., 1982). The assumption for this study is

15 that surface roughness variations play a minor role regarding spatial backscatter differences across the study site. Backscatter increases with increasing vegetation height for X-band in tundra what originates from volume scattering and double bounce (leading to higher backscatter) rather than surface roughness (Ullmann et al., 2014). It can be also expected that soil moisture variations are not reflected in X-band measurements when vegetation cover is present. The assumption is that volume scattering and double bounce in vegetation is the main contributor to spatial differences in backscatter.

20 The local vegetation patterns are influenced by terrain and soil moisture and also correlate with snow cover thickness, which are all ALT influencing factors (Shiklomanov and Nelson, 1999; Gomersall and Hinkel, 2001; Kelley et al., 2004). Areas with shrubs have higher snow cover, which prevents the ground from cooling in the winter. The ALT is therefore also higher than in the surrounding. Based on results of previous studies which utilized the vegetation index NDVI (Table 1) it is expected that a relationship between X-Band backscatter measurements and ALT is given. A data set based on TerraSAR-X which allows

25 the investigation of this relationship has been compiled. This included for SAR common pre-processing steps to account for variations due to viewing geometry.

Six TerraSAR-X images from August 2014 and 2015 were processed (three images per year). It is assumed that within this time stable phenological conditions can be expected. Utilising the software NEST (Next ESA SAR Toolbox) Range-Doppler Terrain Correction was performed with a TanDEM-X Intermediate DEM ($\sim$ 12 m resolution). Images were processed to a pixel

30 spacing of 2 m and a radiometric normalization was applied. The so called resulting σ_0 values were then converted into dB. The term backscatter refers in the following to these values. SAR data are affected by so called speckle which is a noiselike effect. It can be understood as an interference phenomenon due to a number of scatterers within each resolution cell. The images were
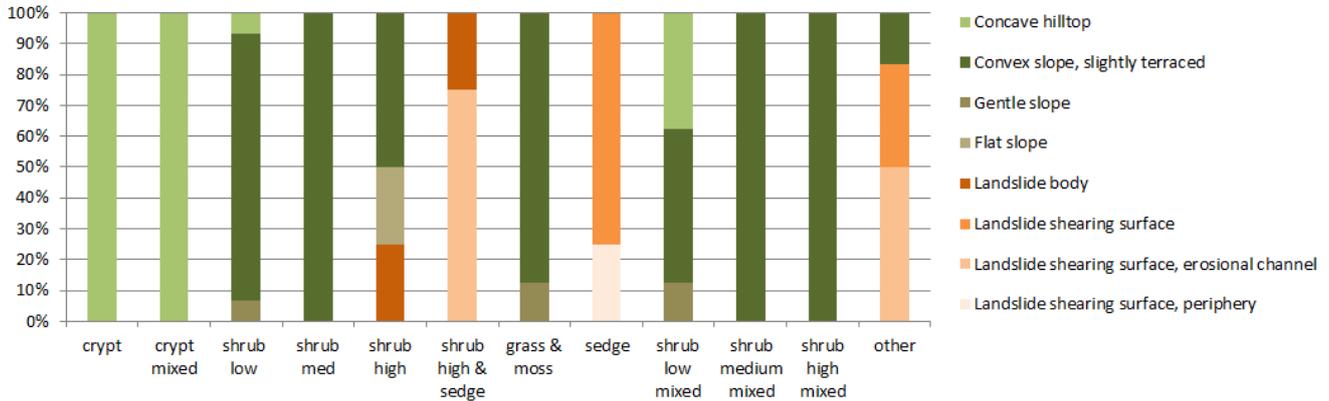
Figure 2. Comparison of topographic units and vegetation type at the CALM grid.

therefore further averaged over time and a spatial filter (5 x 5 mean neighbourhood – 10 m) was applied to account for this noise.

Backscatter as well as NDVI values for the Vaskiny Dachi sites one to three were extracted and compared to the mean ALT values of 2014 and 2015 of each measuring point. σ_0 values have been directly compared to ALT and also statistics for classes

5 of backscatter have been derived (class range 1 dB). These results were then further used in order to determine a relationship allowing the conversion of σ_0 values into ALT values. Three different functions were tested to characterise the relationship between TerraSAR-X backscatter and ALT values. An automatically fitted linear function, an automatically fitted polynomial function and an adapted polynomial function which behaves better for low ALT values where measuring values are missing (see Figure 5). Validation has been undertaken using ALT measurements at the CALM grid. A similar approach was followed

10 for the NDVI records.

Backscatter statistics have been also derived for different vegetation classes from locations of the 2014 survey outside of the ALT measurement sites. These locations represent relatively homogeneous sites (with respect to TerraSAR-X spatial resolution). The ALT sites, especially the CALM grid, are comparably heterogeneous and therefor of limited applicability for determination of backscatter dependence on vegetation type.

4 Results

The assumption that backscatter increases with increasing amount of vegetation could be confirmed for the Vaskiny Dachi area (Figure 3). There is a difference of about 2 dB between the median for shrubs less than 20 cm and those larger than 60 cm. σ_0 values for the grass/sedge class do however exceed these values. Cryptogam crust backscatter is at the same order of magnitude like shrubs between 20 and 60 cm height.

20 Class statistics (Figure 4) indicate a relationship between σ_0 and larger thaw depths (> 70 cm). The median σ_0 for shallow ALT does not decrease with decreasing ALT at the same rate as for deeper ALT.
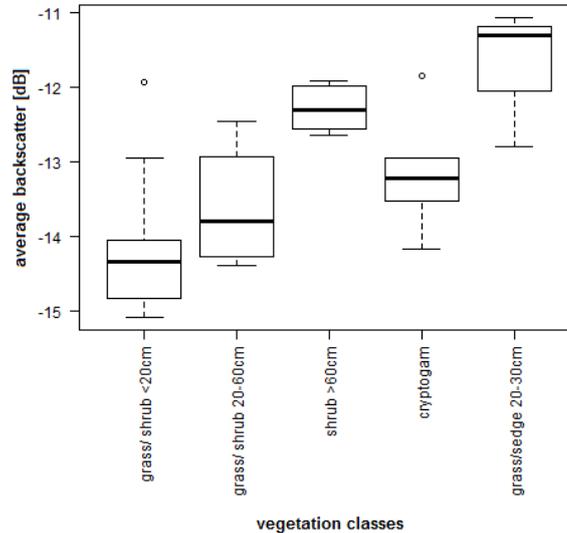
Figure 3. Boxplot for backscatter values of various vegetation types. The used points were recorded within a field campaign in 2014. Backscatter values were extracted from the temporally averaged and spatially filtered image of August 2014 and 2015 acquisitions.

Scatterplots of the filtered σ_0 and ALT values of the sites VD-1 to VD-3 also indicate this correlation (see Figure 5). Comparing all three VD sites it becomes apparent that low backscatter values dominate in areas with low ALT and high backscatter values coincide with high ALT. σ_0 increases with increasing ALT. The overall higher ALT values of VD-3 are reflected by their higher backscatter values. A range of 5 dB can be observed for an ALT range of 100 cm (40 - 140 cm). Some

5 sites show a variability of more than 1 dB between the acquisitions of 2014 and 2015. An exclusion of these points would slightly increase the coefficients of determination, but no positive effect could be found with RMSE values at the CALM grid.

Coefficients of determination of below 0.66 were obtained for all tested functions (see Table 2). The resulting RMS errors at the CALM grid site range from 20 to 22 cm.

The found relationship between TerraSAR-X backscatter and ALT is not that pronounced at the CALM validation site as

10 at the other plots. Especially a patch at the highest elevation of the CALM grid was expected to show higher ALT values according to the calculations from the satellite data (Figure 8 and Figure 6). There are also some spots with slightly higher ALT than predicted. This applies to ALT larger than 125 cm. With the exception of the area around the hilltop the patterns derived with TerraSAR-X however resemble those of the in situ measurements.

A deeper active layer can be found in areas with high shrubs as well as cryptogam crust at the CALM site (see Figure 6).

15 Extremes of ALT can further be encountered at the clay-rich landslides with relatively sparse vegetation, classified as 'other' in Figure 6. Thinner active layers were encountered at zones with grass and moss or low shrubs (see Figure 6). Residuals increase for depths larger than 125 cm, especially in case of dominance of cryptogam crusts.

Derived scatterplots of NDVI and ALT values also reveal a relationship within the observed range of 0.46 – 0.65 (Figure 5). All tested functions showed even greater coefficients of determination of about 0.73 - 0.76, than the TerraSAR-X approach

Table 2. R^2 between X-band backscatter and NDVI (22nd July 2014 and 10th August 2015) respectively and active layer thickness (ALT) from VD-1,2 and 3 for tested functions. RMSE values represent the modelled versus measured ALT at the CALM site.

functions	R^2 (VD-1, 2 and 3)	RMSE [cm] (CALM)
TSX linear	0.656	20
TSX polynomial	0.616 (for σ_0 > -15.2 dB)	22
TSX adapted polynomial	0.457 (for σ_0 > -16 dB)	22
TSX linear (exclusion of points with high variability)	0.712	21
NDVI 22nd July 2014 linear	0.734	27
NDVI 22nd July 2014 polynomial	0.752	29
NDVI 22nd July 2014 polynomial adapted polynomial	0.742	28
NDVI 10th August 2015 linear	0.746	30
NDVI 10th August 2015 polynomial	0.761	31
NDVI 10th August 2015 polynomial adapted polynomial	0.754	30

(Table 2). The achieved RMSE at the validation site is however about 7 cm larger than when using the TerraSAR-X backscatter values. Furthermore, when using only site VD-3, which has the highest range and total thickness of the active layer, the linear regression for the backscatter values has a coefficient of determination of 0.622 while for NDVI values it is only 0.017 and 0.002 respectively (Figure 5). The NDVI derived ALT values for the CALM site range at most between 70 and 100 cm for 22nd July 2014 and between 60 110 cm for 10th August 2015, while measured values have a range of 60 - 150 cm, with values > 130 only found for saline clay (Figure 7).

5 Discussion

X-Band backscatter spatial variations seem to resemble ALT for larger thaw depths only (> 70 cm). There are however differences between the training datasets. Both, VD-1 and VD-2, lie within a similarly lower ALT range, with VD-1 showing slightly lower backscatter values than VD-2. These differences can also be observed for NDVI (Figure 5). Especially the acquisition of 22nd July 2014 shows clearly higher NDVI values for VD-1 than for VD-2. The backscatter differences could be explained due to a slightly higher surface roughness, which is however not pronounced enough to have a sufficient influence on the sites snow cover or even ALT. This is supported by the comparison to vegetation types (Figure 3). Vegetation at VD-2 is very heterogeneous and also includes patches of sedges or reeds. Such sites have higher backscatter than shrub dominated areas. While VD-1 and to a small amount even VD-3 also show sedge vegetation, these sandier sites show a different kind of grass (carex bigelowii instead of calamagrostis holmii).

The assumption that backscatter variations result from mostly differences in volume scattering in vegetation does not seem to be valid for the selected sites. It agrees with findings of McMichael et al. (1997) that the amount of vegetation alone cannot
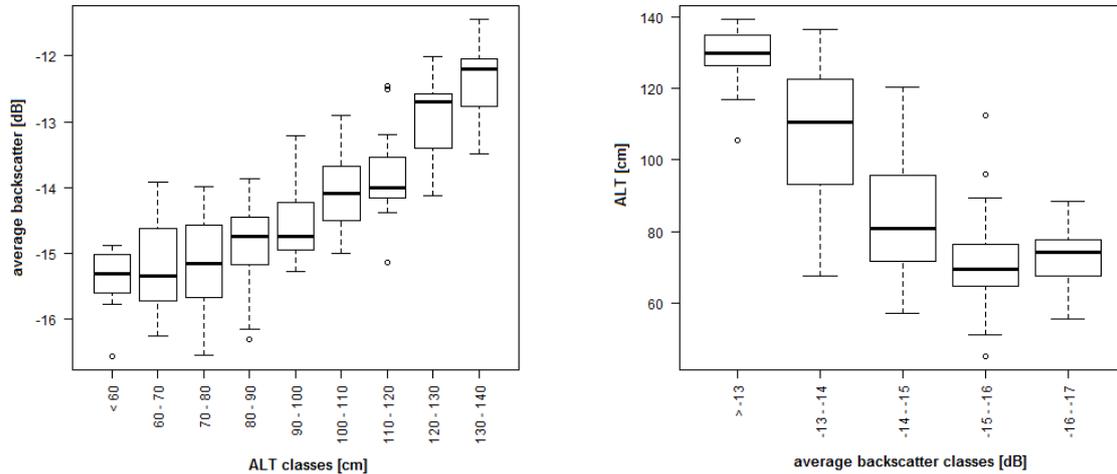
Figure 4. Left: σ_0 statistics for Active Layer Thickness (ALT) classes (10 cm) of the sites VD-1 to VD-3. Right: ALT statistics for backscatter classes (1 dB) of the sites VD-1-3.

be used for ALT retrieval. Using backscatter intensity at only one polarization, does not allow to distinguish between surface and volume scattering. Polarimetric analyses (using other combinations of H and V polarizations) may help to distinguish the scattering mechanism contributions (see e.g. Ullmann et al. (2014)). Data acquired at different polarizations are however not available for the study site.

5   As described in Duguay et al. (2015) areas with high shrubs show higher backscatter values. A pronounced relationship was however not found for X-band in HH by Ullmann et al. (2014) over the MacKenzie Delta. They applied a smaller spatial filter of 3 x 3 and used data from the end of the growing season (mostly September) when plant decay is already expected to take place. Our results however indicate that there is a relationship for the Vaskiny Dachi area (see Figure 3).

The comparison of the produced ALT map to the ALT measurements at CALM grid showed that some points within the
10   validation dataset from the CALM grid are not well represented by the produced ALT map. For instance for one of these points an ALT of > 170 cm was measured in 2014, which is about almost double the values of the surrounding points, and in 2015 only 116 cm were registered. Such an extreme variability of ALT could be explained by an interface between a sandy active layer and a clayey permafrost at this location. In clayey saline soils (as can be found at the study site) the freezing point is different from zero and probes can be inserted to greater depths (Leibman, 1998). On the other hand restrictions of
15   the used approach become apparent. Most points for which the modelled ALT shows high deviations from the in situ data have or lie close to spots of cryptogam crust. These are typically found on the high centred sandy polygons in the study area. The comparably high ALT values are here not driven by trapped snow in winter but higher conductivity of heat throughout the summer. The surface roughness for areas with cryptogam crusts is expected to be comparably low but the recorded σ_0 is comparable to medium shrub heights which have a lower thaw depth. The radar signal may penetrate deeper into the soil
20   surface at such sites depending on moisture content. The moisture content itself may also contribute to σ_0. However in situ
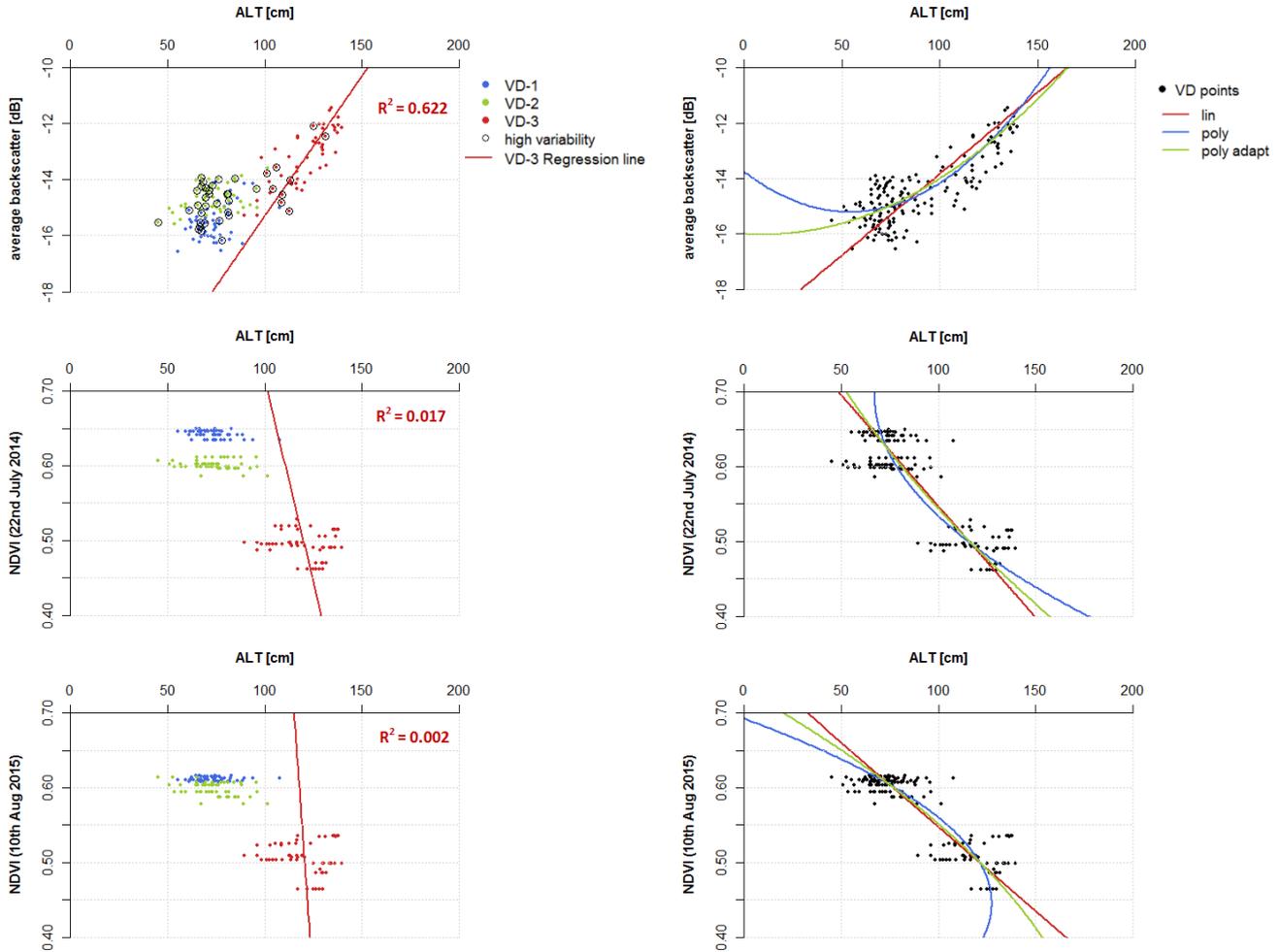
Figure 5. Upper Left: Comparison between σ_0 and Active Layer Thickness (ALT) values at the sites VD-1 to VD-3; points with differences of more than 1 dB between 2014 and 2015 are marked by circles. Linear Regression for site VD-3 for σ_0 and Active Layer Thickness (ALT) values. Middle and bottom left: Comparison between NDVI (22nd July 2014 and 10th August 2015) and Active Layer Thickness (ALT) values at the sites VD-1 to VD-3. Linear Regression for site VD-3 for NDVI and Active Layer Thickness (ALT) values. Upper right: Three different functions fitted to σ_0 and Active Layer Thickness (ALT) values. Middle and bottom right: Three different functions fitted to NDVI (22nd July 2014 and 10th August 2015) and Active Layer Thickness (ALT) values.

soil moisture measurements of the top layer in the overall dry August 2015 showed lowest soil moisture values for areas with cryptogam crust, while the wettest areas were covered with sedges and high shrubs (see Figure 9). Heterogeneity regarding vegetation coverage may also contribute. Especially sites with mixed types show high deviations (see Figure 6).

The comparison to Landsat 8 derived NDVI values demonstrates the advantages and disadvantages of the new approach with respect to previous studies. Investigations presented in this paper showed that the introduced approach of using TerraSAR-X
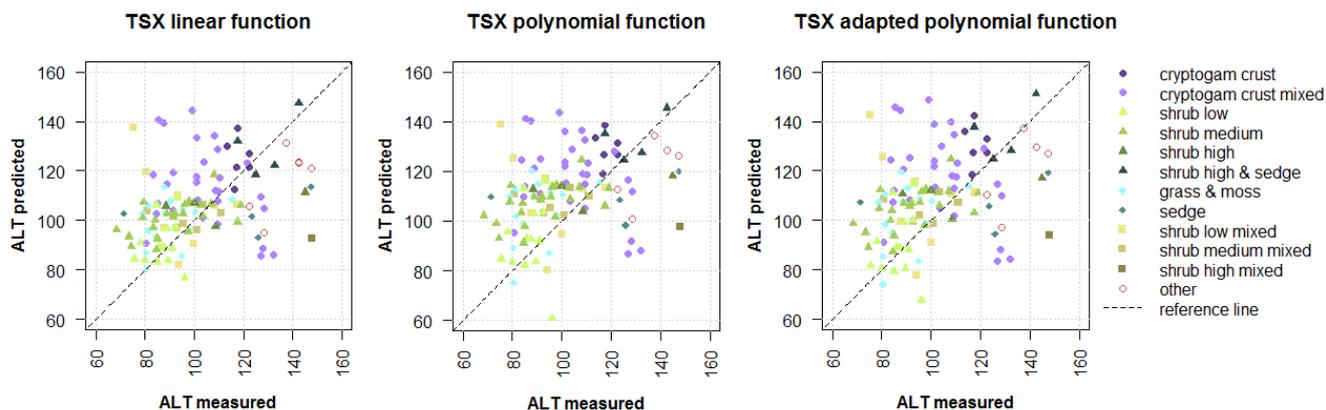
Figure 6. Comparison between predicted and measured ALT values at the CALM grid with differentiation between vegetation types for the three tested backscatter functions.

backscatter values to delineate ALT values is suitable to provide higher than 30 m resolution estimates over unsaturated soils with ALT ranging from 70 cm to 150 cm in areas outside of high centred sandy polygons. One previous study that was conducted within comparable ALT ranges used NDVI and land cover information respectively derived from Landsat data in combination with DEM data to derive three classes of ALT (Leverington and Duguay, 1996). A 93% agreement rate for three different ALT classes was obtained. In difference to our study Leverington and Duguay used "best-estimate" ALT values from either a pit value, or the average of pit and probe measurements. In our study we used measurements for single points from grid points within a 100 x 100 m raster of high heterogeneity. All but one measured ALT values fall into only one ALT class (70 - 150 cm) used by Leverington and Duguay. The given accuracy can therefore not be compared.

Our results confirm that the NDVI can be used to distinguish between lower and higher ALT. NDVI can be however not used to obtain the actual spread of ALT. This might be partially the result of the lower spatial resolution. High spatial resolution satellite data would be required to determine this influence.

The used TerraSAR-X data have been acquired in stripmap mode which has a swath width of 30 km. This sensor can however also acquire data over 270 km when using the Wide ScanSAR mode (40 m resolution). This would allow the transfer of the approach to larger regions.

6 Conclusions

The common dependency of ALT and X-band backscatter values on land cover types as well as the interrelation of terrain, vegetation, soil moisture and snow cover yields a correlation which can be used to derive ALT with an RMSE of 20-22 cm depending on function type. It can be shown that in general higher ALT values corresponded with higher backscatter values. The approach does however seem to be limited to ALT depths larger than 70 cm. The accuracy is lower over sites with mixed
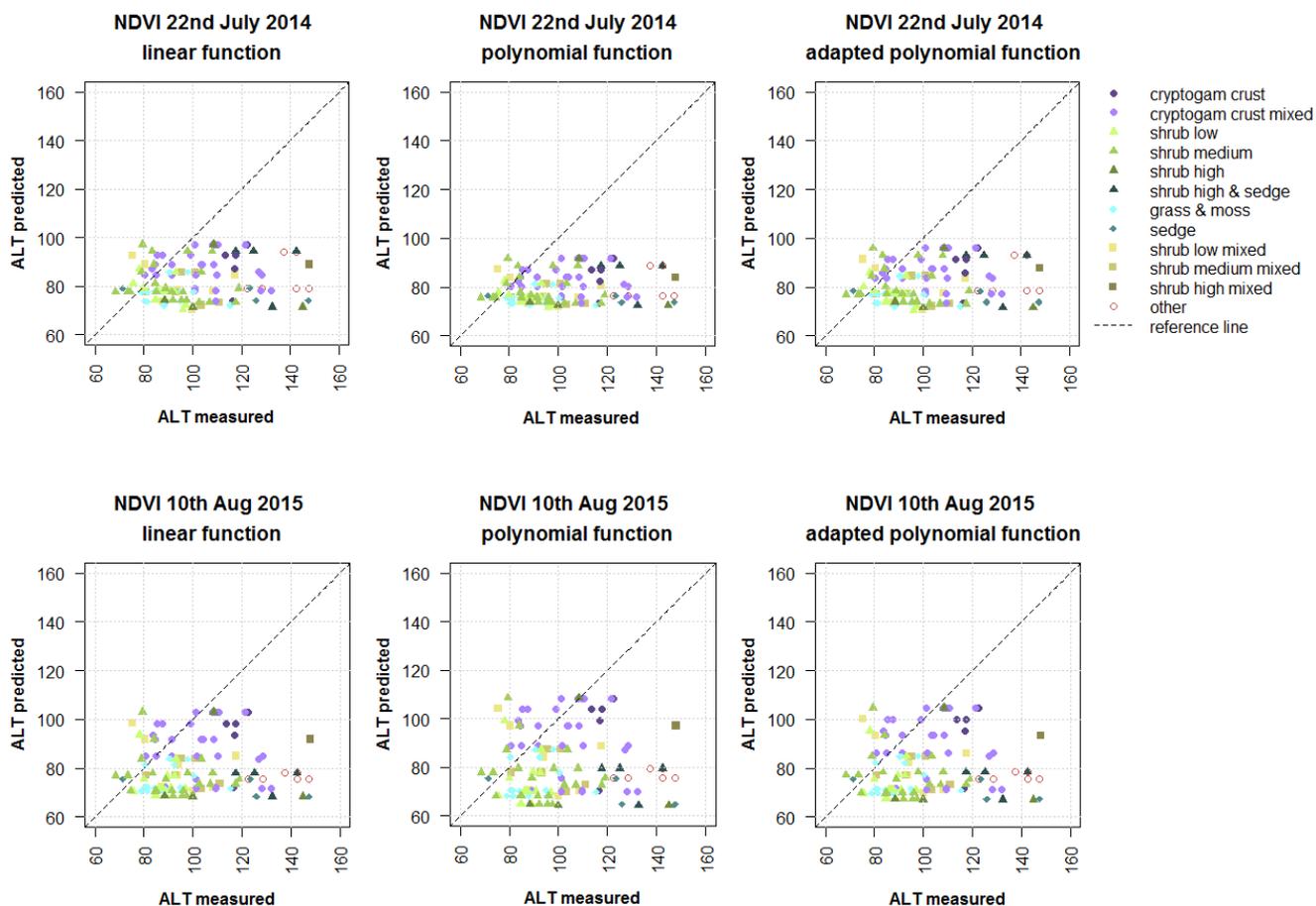
Figure 7. Comparison between predicted and measured ALT values at the CALM grid with differentiation between vegetation types for the three tested NDVI functions for 22nd July 2014 and 10th August 2015.

vegetation types within the pixels. Polarimetric SAR analyses might be suitable to tackle roughness issues. This could however not be tested due to unavailability of such satellite data. Results indicate a better performance than NDVI for higher ALT, but investigations with higher spatial resolution data would be required for confirmation.

Author contributions. Barbara Widhalm has performed all data analyses, collected moisture and vegetation information at the CALM site and compiled the manuscript. Annett Bartsch has been contributing to the development of the concept of the approach as well as to the manuscript. Marina Leibmann and Artem Khomutov have collected the active layer measurements at the long term monitoring sites as well as the vegetation information at sites outside of the ALT monitoring sites and contributed to the interpretation and discussion of the results.
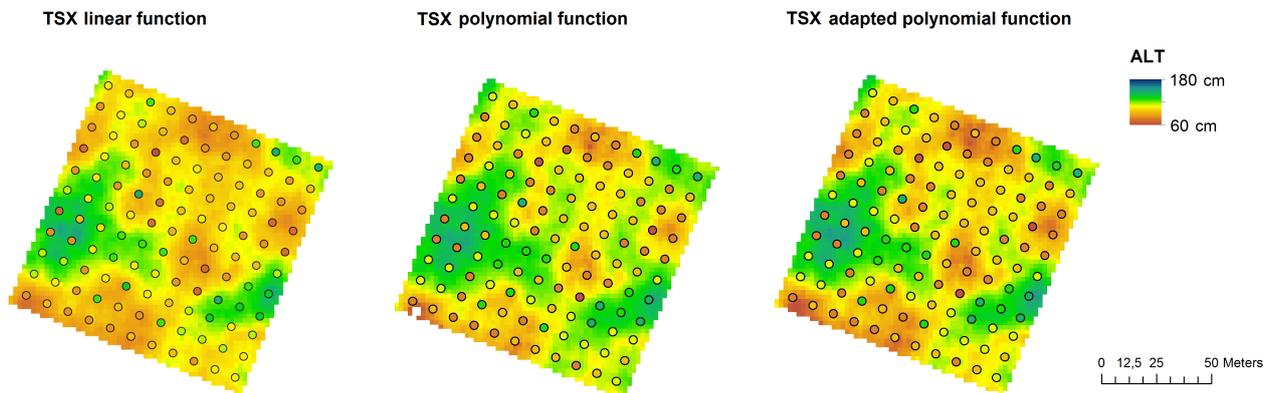
Figure 8. Calculated ALT maps (background raster, based on X-band backscatter) for the CALM grid compared to in situ measurements (circles)
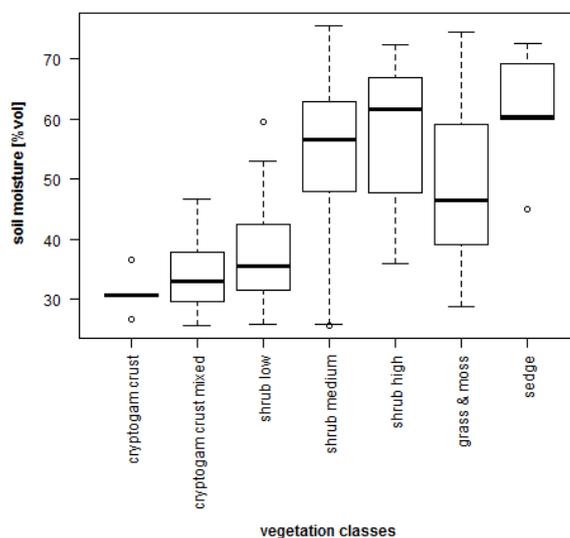
Figure 9. Boxplot for mean soil moisture values of three acquisition dates in late August 2015 for vegetation types at the CALM grid.

Acknowledgements. This work was supported by the Austrian Science Fund under Grant [I 1401] and Russian Foundation for Basic Research Grant 13-05-91001-ANF-a (Joint Russian–Austrian project COLD-Yamal). TerraSAR-X data have been available by DLR through PI agreement LAN1706 and HYD2522, and Tandem-X data through HYDR0226.

References

Brown, J., Hinkel, K. M., and Nelson, F. E.: The circumpolar active layer monitoring (CALM) program: Research designs and initial results, Polar Geography, 24, doi:10.1080/10889370009377698, 2000.

DLR: TanDEM-X: Grround Segment, DEM Products Specification Document.

5 DLR: TerraSAR-X Missiom, brochure, 2009.

Duguay, Y., Bernier, M., Lvesque, E., and Tremblay, B.: Potential of C and X Band SAR for Shrub Growth Monitoring in Sub-Arctic Environments, Remote Sensing, 7, 9410–9430, doi:10.3390/rs70709410, 2015.

Dvornikov, Y., Khomutov, A., Mullanurov, D., Ermokhina, K., Gubarkov, A., and Leibman, M.: GIS and field data based modelling of snow water equivalent in shrub tundra, Fennia, 193, 53–65, doi:10.11143/46363, 2015.

10 Gangodagamage, C., Rowland, J. C., Hubbard, S. S., Brumby, S. P., Liljedahl, A. K., Wainwright, H., Wilson, C. J., Altmann, G. L., Dafflon, B., Peterson, J., Ulrich, C., Tweedie, C. E., and Wullschleger, S. D.: Extrapolating active layer thickness measurements across Arctic polygonal terrain using LiDAR and NDVI data sets, Water Resources Research, 50, 6339–6357, doi:10.1002/2013WR014283, 2014.

Gomersall, C. E. and Hinkel, K. M.: Estimating the Variability of Active-La yer Thaw Depth in Two Physiographic Regions of Northern Alaska, Geographical Analysis, 33, 141–155, 2001.

15 Harlan, R. and Nixon, J. F.: Geotechnical engineering for cold regions, chap. Ground thermal regime, pp. 103–163, McGraw-Hill Book Co., New York, N.Y., United States, 1978.

Harris, S., French, H., Heginbottom, J., Johnston, G., Ladanyi, B., Sego, D., and van Everdingen, R.: Glossary of Permafrost and Related Ground-Ice Terms, National Research Council of Canada, Ottawa. Technical Memorandum 142, 1988.

Hinkel, K. M. and Nelson, F. E.: Spatial and temporal patterns of active-layer thickness at Circumpolar Active-Layer Monitoring (CALM)
20 sites in Northern Alaska, 19952000, Journal of Geophysical Research, 108, doi:10.1029/2001JD000927, 2003.

Huggett, R. J.: Fundamentals of Geomorphology, Routledge, 2 edn., 2007.

IPCC: Climate Change 2013: The Physical Science Basis. Contribution of Working Group I to the Fifth Assessment Report of the Intergovernmental Panel on Climate Change, Cambridge University Press, Cambridge, United Kingdom and New York, NY, USA, doi:10.1017/CBO9781107415324, 2013.

25 Kane, D. L., Hinzman, L. D., and Zarling, J.: Thermal Response of the Active Layer to Climatic Warming in a Permafrost Environment, Cold Regions Science and Technology, 19, doi:10.1016/0165-232X(91)90002-X, 1991.

Kelley, A. M., Epstein, H. E., and Walker, D. A.: Role of vegetation and climate in permafrost active layer depth in arctic tundra of northern Alaska and Canada, Journal of Glaciology and Climatology, 26, 269–273, 2004.

Khomutov, A. and Leibman, M.: Landslides in Cold Regions in the Context of Climate Change, chap. Assessment of Landslide Hazards in
30 a Typical Tundra of Central Yamal, Russia, pp. 271–290, Springer International Publishing, doi:10.1007/978-3-319-00867-7_20, 2014.

Krieger, G., Moreira, A., Fiedler, H., Hajnsek, I., Werner, M., Younis, M., and Zink, M.: TanDEM-X: A Satellite Formation for High-Resolution SAR Interferometry, IEEE Trans. Geosci. Remote Sens., 45, doi:10.1109/TGRS.2007.900693, 2007.

Kudryavtsev, V. A., Garagulia, L., Kondratyeva, K. A., and Melamed, V. G.: Fundamentals of Frost Forecasting in Geological Engineering Investigations, Nauka, Moscow. Draft Translation 606, Cold Regions Research And Engineering Lab Hanover N H, 1974.

35 Leibman, M., Moskalenko, N., Orekhov, P., Khomutov, A., Gameev, I., Khitun, O., Walker, D., and Epstein, H.: Polar cryosphere of water and land, chap. Interrelation of cryogenic and biotic components of geosystems in cryolithozone of West Siberia on the Transect Yamal", p. 171192, Paulsen Publisher, Moscow, 2011.

Leibman, M., Khomutov, A., Orekhov, P., Khitun, O., Epstein, H., Frost, G., and Walker, D.: Gradient of seasonal thaw depth along the Yamal transect, in: Proceedings of the tenth international conference on permafrost; translation of Russian contributions, edited by Melnikov, V., Drozdov, D., and Romanovksy, V., vol. Vol.10(Volume 2), pp. 237–242, 2012.

Leibman, M., Khomutov, A., Gubarkov, A., Mullanurov, D., and Dvornikov, Y.: The research station Vaskiny Dachi, Central Yamal, West Siberia, Russia A review of 25 years of permafrost studies, Fennia, 193, 3–30, doi:10.11143/45201, 2015.

Leibman, M. O.: Thaw depth measurements in marine sailne sandy and clayey deposits of Yamal peninsula, Russia: procedure and interpretation of results, in: PERMAFROST - Seventh International Conference (Proceedings), Yellowknife (Canada), Collection Nordicana, 55, pp. 635–639, 1998.

Leverington, D. W. and Duguay, C. R.: Evaluation of Three Supervised Classifiers in Mapping Depth to Late-Summer Frozen Ground, Central Yukon Territory, Canadian Journal of Remote Sensing, 22, doi:10.1080/07038992.1996.10874650, 1996.

McMichael, C. E., Hope, A. S., Stow, D. A., and Fleming, J. B.: The relation between active layer depth and a spectral vegetation index in arctic tundra landscapes of the North Slope of Alaska, International Journal of Remote Sensing, 18, doi:10.1080/014311697217666, 1997.

Melnikov, E. S., Leibman, M. O., Moskalenko, N. G., and Vasiliev, A. A.: Active-Layer Monitoring in the Cryolithozone Of West Siberia, Polar Geography, 28, 267–285, doi:10.1080/789610206, 2004.

Nelson, F. E., Shiklomanov, N. I., Mueller, G. R., Hinkel, K. M., Walker, D. A., and Bockheim, J. G.: Estimating Active-Layer Thickness over a Large Region: Kuparuk River Basin, Alaska, U.S.A., Arctic and Alpine Research, 29, doi:10.2307/1551985, 1997.

Peddle, D. R. and Franklin, S. E.: Classification of permafrost active layer depth from remotely sensed and topographic evidence, Remote Sensing of Environment, 44, doi:10.1016/0034-4257(93)90103-5, 1993.

Permafrost Subcommittee, A. C. o. G. R.: Glossary of Permafrost and Related Ground-Ice Terms, National Research Council of Canada, Ottawa. Technical Memorandum, 1988.

Sazonova, T. S. and Romanovsky, V. E.: A model for regional-scale estimation of temporal and spatial variability of active layer thickness and mean annual ground temperatures, Permafrost and Periglacial Processes, 14, 125–139, doi:10.1002/ppp.449, 2003.

Schaefer, K., Liu, L., Parsekian, A., Jafarov, E., Chen, A., Zhang, T., Gusmeroli, A., Panda, S., Zebker, H. A., and Schaefer, T.: Remotely Sensed Active Layer Thickness (ReSALT) at Barrow, Alaska Using Interferometric Synthetic Aperture Radar, Remote Sensing, 7, 3735–3759, doi:10.3390/rs70403735, 2015.

Shiklomanov, N. I. and Nelson, F. E.: Analytic representation of the active layer thickness field, Kuparuk River Basin, Alaska, Ecological Modelling, 123, doi:10.1016/S0304-3800(99)00127-1, 1999.

Smith, M.: Potential Responses of Permafrost to Climatic Change, Journal of Cold Regions Engineering, 4, 29–37, 1990.

Ulaby, F. T., Moore, R. K., and Fung, A.: Microwave Remote Sensing–Active and Passive, vol. II, Artech House, Norwood, Mass., 1982.

Ullmann, T., Schmitt, A., Roth, A., Duffe, J., Dech, S., Hubberten, H.-W., and Baumhauer, R.: Land Cover Characterization and Classification of Arctic Tundra Environments by Means of Polarized Synthetic Aperture X- and C-Band Radar (PolSAR) and Landsat 8 Multispectral Imagery Richards Island, Canada, Remote Sensing, 6, 8565–8593, doi:10.3390/rs6098565, 2014.

Vasiliev, A. A., Leibman, M. O., and Moskalenko, N. G.: Active Layer Monitoring in West Siberia under the CALM II Program, in: Proceedings of the Ninth International Conference on Permafrost, edited by Kane, D. L. and Hinkel, K. M., vol. 2, p. 18151820, Institute of Northern Engineering, University of Alaska Fairbanks, 2008.

Walker, D., Epstein, H., Leibman, M., Moskalenko, N., Orekhov, P., Kuss, J., Matyshak, G., Kaarlejrvi, E., Forbes, B., Barbour, E., and Gobroski, K.: Data Report of the 2007 and 2008 Yamal Expeditions, Alaska Geobotany Center, Institute of Arctic Biology, University of Alaska Fairbanks, Fairbanks, AK. 121 pp., 2009.

Werninghaus, R., Balzer, W., Buckreuss, S., Mittermayer, J., and Mhlbauer, P.: The TerraSAR-X Mission, in: SPIE 5236, SAR Image Analysis, Modeling, and Techniques VI, doi:10.1117/12.511500, 2004.

Yershov, E. D.: General Geocryology, Cambridge University Press, Cambridge, 1998.